

Harnessing sparsity in lamb wave-based damage detection for beams

Debarshi Sen^{1a}, Satish Nagarajaiah^{*1,2} and S. Gopalakrishnan^{3b}

¹Department of Civil and Environmental Engineering, Rice University, 6100 Main Street, MS 318, Houston, TX 77005, USA

²Department of Mechanical Engineering, Rice University, 6100 Main Street, MS 318, Houston, TX 77005, USA

³Department of Aerospace Engineering, Indian Institute of Science, CV Raman Road, Bangalore 560012, India

(Received November 6, 2017, Revised November 21, 2017, Accepted November 23, 2017)

Abstract. Structural health monitoring (SHM) is a necessity for reliable and efficient functioning of engineering systems. Damage detection (DD) is a crucial component of any SHM system. Lamb waves are a popular means to DD owing to their sensitivity to small damages over a substantial length. This typically involves an active sensing paradigm in a pitch-catch setting, that involves two piezo-sensors, a transmitter and a receiver. In this paper, we propose a data-intensive DD approach for beam structures using high frequency signals acquired from beams in a pitch-catch setting. The key idea is to develop a statistical learning-based approach, that harnesses the inherent sparsity in the problem. The proposed approach performs damage detection, localization in beams. In addition, quantification is possible too with prior calibration. We demonstrate numerically that the proposed approach achieves 100% accuracy in detection and localization even with a signal to noise ratio of 25 dB.

Keywords: sparsity; lamb waves; damage detection; statistical learning

1. Introduction

Structural health monitoring (SHM) is a necessity for continuity of functionality of engineering and infrastructure systems (Boller 2000, Ou and Li 2010). It typically entails deployment of an array of sensors on a system of interest for continuous data acquisition, using which one may perform damage detection, followed by estimation of remaining useful life (Farrar and Worden 2007). Rytter (1993) classifies damage detection into four different levels, I through IV. Level I is the determination of existence of damage, level II is damage localization, level III is quantification of damage and level IV is associated to estimation of remaining useful life.

We may classify damage detection based on the approach as active or passive. As the names suggest, active damage detection involves actuating a system of interest with an external load prior

*Corresponding author, Ph.D., E-mail: satish.nagarajaiah@rice.edu

^aE-mail: debarshi.sen@rice.edu

^bPh.D., E-mail: gopal@iisc.ernet.in

to data acquisition. Passive damage detection, on the other hand, involves data acquisition from the system based on ambient excitations of the system itself. Another way of classifying damage detection is the frequency content of time history signals that we acquire from a system. Signal acquisition in the low frequency and high frequency regimes are called vibration-based (Farrar *et al.* 2001) and guided wave-based techniques (Rose 2004), respectively. In this paper we focus on guided wave-based active damage detection in beams.

The increase in popularity of the use of guided waves for damage detection owes to their sensitivity to small damages over a considerable distance (Raghavan and Cesnik 2007). Guided waves are high frequency waves (frequency in the order of 100 to 1000 kHz), that propagate through a continuous medium. Some of the most popular theoretical treatise of the subject can be found in Graff (1991), Rose (1999) and Doyle (1997). Damage detection using such waves typically entails the understanding of the signal features that a damage may induce (Alleyne *et al.* 1998, Demma *et al.* 2004).

Use of guided ultrasonic waves is prevalent in many structural and aerospace applications. They are typically used for defect detection in plate (Yu *et al.* 2011, Giurgiutiu 2008, Lu *et al.* 2007) and pipe (Lowe *et al.* 1998, Park *et al.* 1996, Na and Kundu 2002) structures. A summary of all such applications may be found in Liu and Kleiner (2012). However, all these methods are typically model-based. This implies it requires construction of high fidelity models or development of theoretical models for comparing with acquired data for the purposes of damage detection. Both high fidelity models and theoretical models may fail to capture all the physics involved in system. In addition, high-fidelity models are typically computationally prohibitive. For example, the application of finite element methods require a large number of elements in order to obtain reliable response estimates in the high frequency domain (Gopalakrishnan 2009). An alternative is to use signal-based or data-driven techniques.

Data-driven techniques do not require assumptions about the system and captures all the physics involved in the system. Such an approach typically constructs a parametric meta-model from data, that does not necessarily mimic system behavior, but performs damage detection efficiently. This idea has led to the applications of statistical/machine learning algorithms in SHM (Worden and Manson 2007, Nagarajaiah and Yang 2017). Statistical learning algorithms are a potent tool for development of parametric models from data (Hastie *et al.* 2009). They are widely used for SHM and damage detection applications. For example, Yang and Nagarajaiah (2014b) use independent component analysis and sparse regression-based approaches (Yang and Nagarajaiah 2013, 2014a) to damage detection involving vibration-based techniques. Recently, statistical learning algorithms have gained popularity in the guided wave-based SHM and damage detection community too (Lu and Michaels 2008, Liu *et al.* 2015, Ying *et al.* 2013a, b, Tibaduiza *et al.* 2013, Tse and Wang 2013, Eybpoosh *et al.* 2016).

In this paper we propose a statistical learning-based approach that harnesses the inherent sparsity in a beam damage detection problem using guided-ultrasonic waves. We propose a sparse representation framework for damage detection. We test the proposed approach for various scenarios that may be encountered in the field. For demonstrating the efficacy of the proposed approach, we use a hybrid spectral finite element method for simulations (Hu *et al.* 2007). This involves a combination of the traditional finite element method (FEM) and the novel spectral finite element method (SFEM) (Gopalakrishnan *et al.* 2007).

2. Sparse representation framework for damage detection

In this section we propose the sparse representation (SR) framework for damage detection. The key idea behind the SR framework is a dictionary matrix \mathbf{A} , for a given beam. Each column of the matrix \mathbf{A} represents a signal retrieved from the beam due to presence of damage at a single location, for a specific actuation signal. For each signal we perform baseline subtraction (subtraction of an a priori acquired undamaged signal) in addition to time windowing, prior to inclusion in the dictionary. The time windowing allows us to focus on damage signatures better. The choice of the time window depends on the geometry of the structure and approximate estimates of group wave velocities in the material.

For p damage locations and time-windowed signal length n , we have the dictionary matrix $\mathbf{A} \in \mathbb{R}^{n \times p}$. This implies the first column of \mathbf{A} , $\mathbf{a}_1 \in \mathbb{R}^{n \times 1}$ is a signal acquired from the beam when there is damage at location 1. Similarly the second column of \mathbf{A} , $\mathbf{a}_2 \in \mathbb{R}^{n \times 1}$ is a signal acquired from the beam when there is a damage at location 2 and so on. Hence, $\mathbf{A} = [\mathbf{a}_1 \ \mathbf{a}_2 \ \dots \ \mathbf{a}_p]$. As discussed earlier, the dictionary matrix is a representative of the beam in terms of its damaged and undamaged states.

Now, let us assume we acquire a background subtracted and time-windowed signal, $\mathbf{y} \in \mathbb{R}^{n \times 1}$ from a case when there is damage at location m , where $1 \leq m \leq p$. This signal can then be represented as

$$\mathbf{y} = \mathbf{A}\mathbf{x} \tag{1}$$

where $\mathbf{x} \in \mathbb{R}^{p \times 1}$ is a vector such that $x_i = 0 \ \forall \ i \neq m$ and $x_m = 1$. A vector like \mathbf{x} where most of the elements are zero is referred to as a sparse vector. Mathematically, a vector of length n is defined as k -sparse *iff* there are only k nonzero elements such that $k \ll n$. Typically the number of damage locations in a system is low, hence the vector \mathbf{x} will typically be sparse. In addition, if \mathbf{y} is acquired from a undamaged case, it will be a vector of zeros, implying that \mathbf{x} will also be a vector of zeros. Equation 1 is the SR framework for damage detection in beams. Henceforth, we will refer to the vector \mathbf{x} as the damage pointer vector as it aids in localization. Hence, using equation 1 we perform both level I and level II damage detection. If vector \mathbf{x} has non-zero entries, we establish the presence of damage. The location of the non-zero element helps carry out damage localization. For multiple damages, there will be multiple nonzero elements in \mathbf{x} . However, this assumption holds only when the damages are small and the effects of multiple damages can be linearly combined (Levine and Michaels 2013). In addition, the number of damages should be such that the sparsity condition on vector \mathbf{x} holds.

Given this framework, one needs to solve for \mathbf{x} from the linear system of equations $\mathbf{y} = \mathbf{A}\mathbf{x}$, under the assumption that \mathbf{x} is sparse. This problem is formulated as an optimization problem as follows (Candes and Romberg 2005)

$$\underset{\mathbf{x}}{\text{minimize}} \|\mathbf{x}\|_0 \text{ such that } \mathbf{y} = \mathbf{A}\mathbf{x}, \tag{2}$$

where $\|\cdot\|_0$ is the ℓ_0 -norm that counts the number of nonzero elements in a vector. In addition to being non-convex, Equation 2 is also numerically unstable and NP complete. Solving it entails enumeration of all $\binom{p}{k}$ possible locations of nonzero entries of \mathbf{x} , if \mathbf{x} is k -sparse Baraniuk (2007). To

overcome these issues, equation (2) is typically reformulated in a ℓ_1 -norm minimization framework (also popularly referred to as the relaxation of ℓ_0 norm to ℓ_1 norm), generally referred to as a *basis pursuit* problem (Candes and Romberg 2005)

$$\underset{\mathbf{x}}{\text{minimize}} \|\mathbf{x}\|_1 \text{ such that } \mathbf{y} = \mathbf{A}\mathbf{x}, \quad (3)$$

where $\|\cdot\|_1$ is the ℓ_1 -norm defined as $\|\mathbf{x}\|_1 = \sum_{i=1}^n |x_i|$ for any vector $\mathbf{x} \in \mathbb{R}^{n \times 1}$, where $|\cdot|$ computes the absolute value of its argument. The computational complexity of the above problem is $\mathcal{O}(p^3)$. To take into account the effects of noise, equation 3 is further modified as:

$$\underset{\mathbf{x}}{\text{minimize}} \|\mathbf{x}\|_1 \text{ such that } \|\mathbf{y} - \mathbf{A}\mathbf{x}\|_2 \leq \epsilon, \quad (4)$$

where ϵ is a measure of the noise. This framework has been used earlier for various classes of problems over of a wide spectrum of engineering fields like face recognition (Yang *et al.* 2010) and medical imaging (Kandel *et al.* 2013). As discussed earlier, the ℓ_1 minimization framework has also been used for vibration-based damage detection purposes earlier (Yang and Nagarajaiah 2013, 2014a, Hernandez 2014). In this paper, we extend the application of this framework to high frequency ultrasonic wave-based damage detection.

To obtain solutions to Eqs. 3 and 4 pursuit algorithms are typically used. Alternatively, one may reformulate the problem as a sparse regression problem and use the LASSO (a regularized linear regression technique used for sparse regression) (Hastie *et al.* 2009) technique as follows

$$\underset{\mathbf{x}}{\text{minimize}} \|\mathbf{y} - \mathbf{A}\mathbf{x}\|_2^2 + \lambda \|\mathbf{x}\|_1, \lambda > 0, \quad (5)$$

where $\|\cdot\|_2$ is the ℓ_2 -norm (for any vector $\mathbf{x} \in \mathbb{R}^{n \times 1}$, $\|\mathbf{x}\|_2 = \sqrt{\sum_{i=1}^n |x_i|^2}$) and λ is the regularization parameter governing the degree of sparsity in vector \mathbf{x} . This can be looked at as a Lagrange multiplier form of equation (4). A detailed description of the LASSO can be found in (Tibshirani 1996). In this paper, we use the `l1ls` solver developed by (Kim *et al.* 2007) for LASSO implementation.

Based on the above discussion, it becomes clear that, for an effective implementation of the proposed algorithm an inherent assumption about the system is made: the damage locations used for dictionary construction are sufficient for effectively characterizing any damage to the system. Under this assumption, we will numerically demonstrate the efficacy of the proposed algorithm when the test vector \mathbf{y} is obtained from scenarios of single damage but different extents to that used for dictionary construction and multiple damages.

3. Simulations

In this work, we perform DD on a homogeneous and isotropic cantilever Timoshenko beam. We perform simulations to demonstrate our sparsity-based approach. Multiple simulation techniques for wave propagation problems are available in the literature. Traditional FEM is one of the most popular approaches owing to its ubiquity and ability of modeling complex systems. However, it has its drawbacks when applied to this class of problems (Gopalakrishnan 2009). In order to obtain accurate simulation results, the element size for a FEM simulation needs to be at least 10 times smaller than the wavelength of the waves expected to propagate in the system. This makes FEM computationally

inefficient. In addition to the traditional FEM, the Boundary Element Method (BEM) has also been employed to tackle these problems (Rose 1999). The Spectral Element Method in time domain proposed by Patera (1984) is another popular means of simulation. Extensions of this method have been used for both two dimensional and three dimensional wave propagation simulations (Ostachowicz *et al.* 2012). These techniques use a special class of shape functions belonging to the orthogonal Legendre polynomials and use Gauss-Lobatto-Legendre points for numerical integration. Consequently, this improves the computational efficiency compared to traditional FEM.

The class of Spectral Element Methods (SEM) developed by Doyle (1997), improves the computational efficiency further for a limited class of problems. The spectral finite element method (SFEM) is an extension of the SEM developed by Doyle with improvements in terms of numerical computations involved for solving eigenvalue problems inherent in this method (Gopalakrishnan *et al.* 2007). Other methods worthy of mention, used for solving these problems are the Finite Difference Method (FDM) and the Local Interaction Simulation Approach (LISA). LISA was developed for ease of computation using supercomputers. Applications of LISA for solving Lamb wave propagation problems are available in the literature using GPU-based systems (Packo *et al.* 2012).

SFEM however, has it's own drawbacks. For example, using SFEM, damage can only be modeled approximately, whereas in traditional FEM it can be captured much more accurately. Although, Chakraborty and Gopalakrishnan (2006) and Kumar *et al.* (2004) model damages in beams and plates using SFEM, without taking aid of traditional FEM, calibrations with traditional FEM is necessary to characterize such approximate damages. SFEM also fails when it comes to modeling complex geometries (Doyle 1997, Gopalakrishnan *et al.* 2007). A combination of traditional FEM and SFEM can overcome such design issues with satisfactory results (Gopalakrishnan and Doyle 1995, Hu *et al.* 2007). We use this hybrid SFEM, which we will refer to as HFEM henceforth, for all simulations in this work. Fig. 1 shows the idea behind HFEM. In this paper, we model the damage in a beam as a rectangular notch crack.

The original SFEM utilizes a Fourier transform-based frequency domain analysis. A drawback of Fourier transform-based SFEM is the fact that it suffers from *wrap around* effect (Doyle 1997). Wrap around is the phenomena that occurs when the time vector considered for the Fourier Transform is not long enough and low frequency components wrap around the signal and corrupt the initial portion. One way of overcoming this is to take longer time windows. However, that will only increase the computational effort involved. The other issue involved with Fourier Transform based SFEM is the fact that a fixed end (no displacement and rotations at the boundary) boundary condition cannot be simulated (Doyle 1997, Gopalakrishnan *et al.* 1992). It is normally approximated by adding a semi infinite element (also known as a throw off element) with very high stiffness (Gopalakrishnan

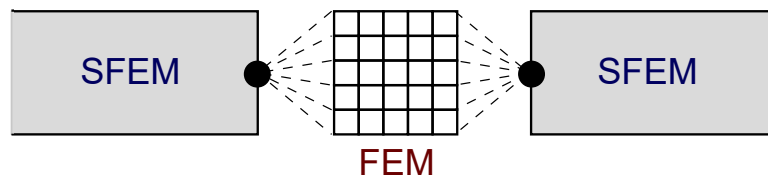


Fig. 1 A schematic showing the ideology behind HFEM. Kinematic relationships are developed between the nodes of SFEM and FEM elements.

et al. 1992). Wavelet Transform based SFEM has been proposed to overcome the wrap around issue (Gopalakrishnan and Mitra 2010), however the accuracy of the frequency domain is lost using the wavelet based SFEM. A Laplace Transform based SFEM has been shown to be the most efficient in overcoming all these (Igawa *et al.* 2004, Murthy *et al.* 2011) drawbacks, and hence has been used for this work.

4. Numerical studies

4.1 Setup

For our simulations we consider a isotropic cantilever beam with Young's modulus $E = 210 \text{ GPa}$, shear modulus $G = 79.3 \text{ GPa}$, mass density $\rho = 7860 \text{ kg/m}^3$, span 2 m and a square cross section of side 20 mm . We model damage as cracks that are 5 mm deep and 2 mm wide. Throughout this work, we treat the width of the crack as a constant. We vary damage extent by changing the crack depth only. As discussed earlier, for modeling a damaged beam, we use a HFEM approach. This involves modeling a FEM based crack system and incorporating it in the SFEM formulation, as described in section 3. For the dictionary, we assume 9 possible locations for damage, they are located at every 200 mm along the length of the beam, as shown in Fig. 2. The damage closest to the fixed end is damage location 1 and the one closest to the free end is damage location 2. Fig. 2 shows all the possible damage locations used to construct the dictionary, \mathbf{A} .

We assume that both the transmitter and the receiver are attached at the free end of the beam, as shown in Fig. 2. We excite the beam using a 5 cycle modulated tone burst with a central frequency of 50 kHz . Fig. 3 shows the time and frequency domain representation of this load. The central frequency is chosen such that the frequency-thickness value is less than the cut-off value for shear modes to be activated. This ensures that we have only one propagating wave mode in the system.

Fig. 4 shows a comparison between a damaged and an undamaged signal obtained from simulation. The wave packet generated due to the presence of damage at location 8 is clearly visible. We further enhance the clarity of this damage feature by performing background subtraction.

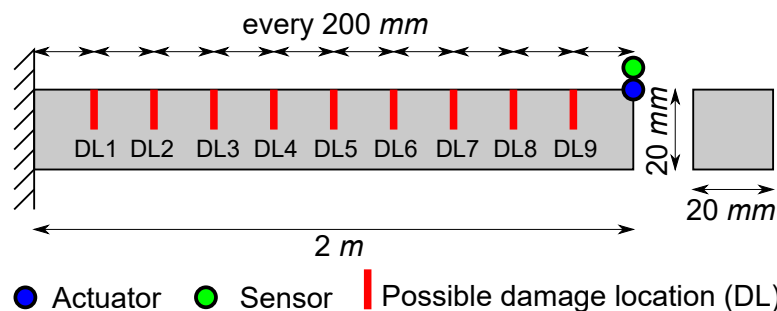


Fig. 2 A schematic of the simulated beam. The red lines are the possible damage locations. We use signals from these locations to construct the dictionary \mathbf{A} from Eq. 1

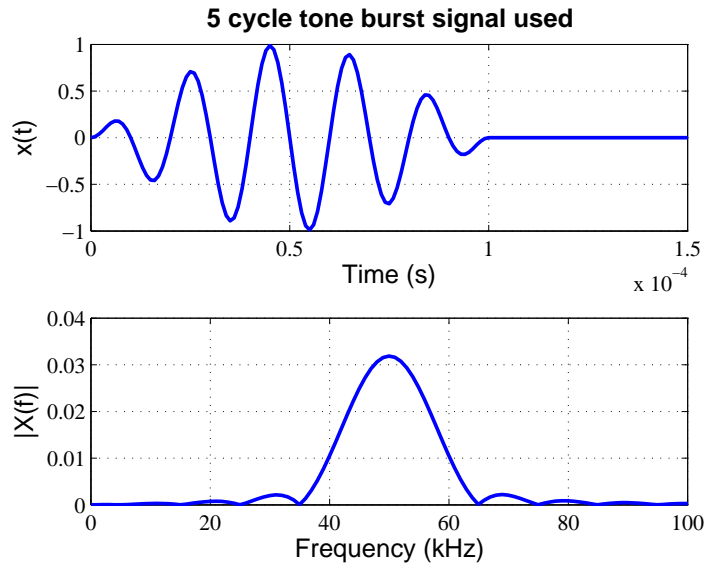


Fig. 3 The time and frequency domain representation of the actuation load we use in this study. This is a 5 cycle tone burst with a central frequency of 50 kHz

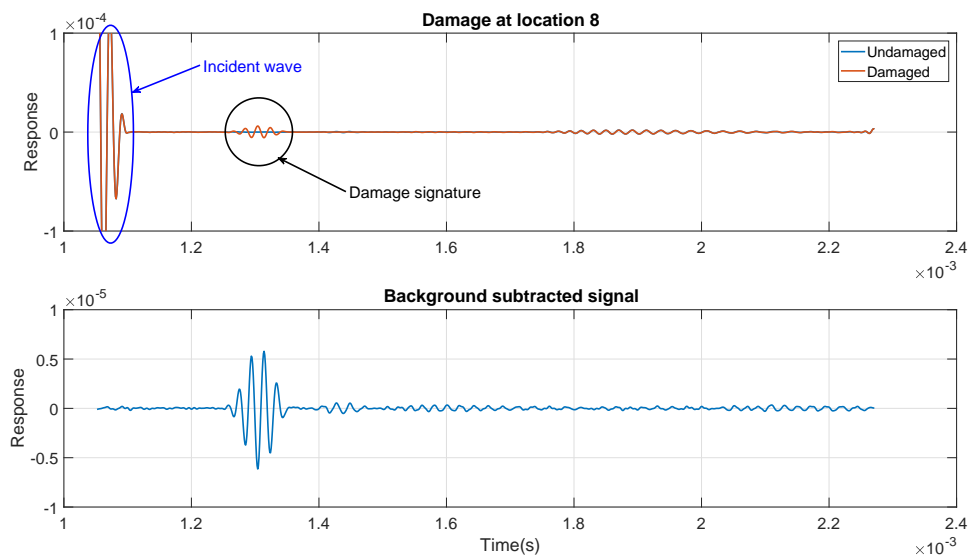


Fig. 4 A comparison of damaged and undamaged signals. We show a time windowed version of the simulated signals. The second figure shows the background subtracted signal, that enhances the damage feature

4.2 Results: Noise free

The first step is to create a dictionary of signals containing information of various damage signatures. We construct a dictionary with a damage size of 2 mm depth. Fig. 5 shows the acquired

signals from the grid locations, namely damage locations 1 through 9.

Fig. 5 shows the signals acquired at the grid locations defined earlier. The image at the top shows the full time history. The first wave packet at around 0.001 *sec* is the incident signal. The subsequent wave packets are the reflections from the fixed end. The lower image shows a time-windowed magnified version of the full time history. This allows us to observe the damage signatures for each of the nine grid locations. These damage signatures are crucial for the functioning of the proposed algorithm.

As discussed earlier, we use background subtracted signals for the dictionary. This helps enhance the damage features. Fig. 6 shows the dictionary elements after background subtraction. Clearly we observe that the damage features are two orders of magnitude smaller than the incident signal. We will use this fact later when dealing with multiple damages.

4.2.1 Case 1: Test signals have the same damage extent as in the dictionary

In this case, we assume that the test signal is from a scenario where the damage extent is the same as that used to construct the dictionary. The purpose of this case is to demonstrate the working of the proposed approach.

Fig. 7 shows the absolute values of the elements of the damage pointer vector, \mathbf{x} . Fig. 7(a) shows the results when the test signal is acquired from a scenario where there is a damage at location 8. So for a single damage scenario the vector \mathbf{x} is 1-sparse. Fig. 7(b) shows the results when the test signal is from an undamaged scenario. As expected, all the elements of the vector \mathbf{x} are zeros. Fig. 8 shows the absolute values of the vector \mathbf{x} for all possible damage locations. We observe that the proposed approach accurately points to the damage location.

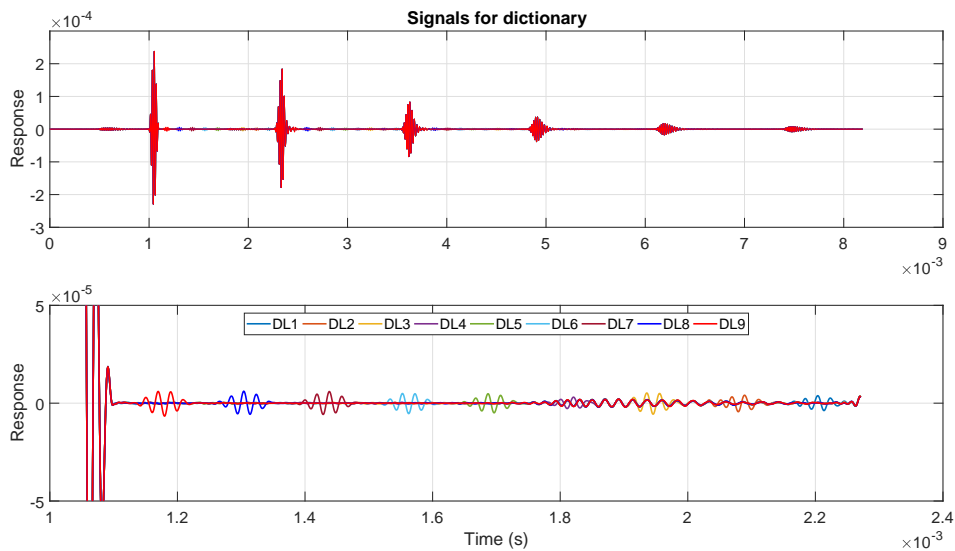


Fig. 5 The time signals acquired at the various grid locations for the dictionary. DL: Damage location

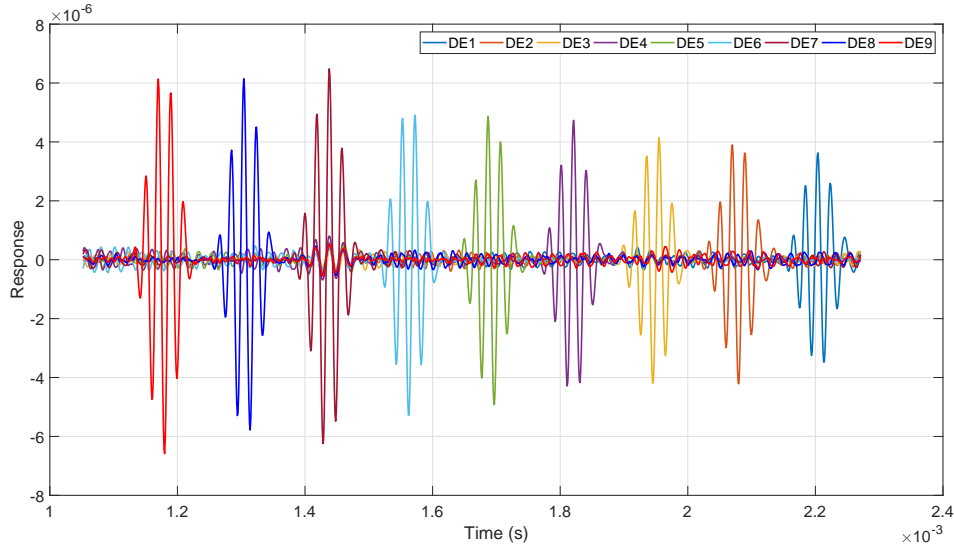


Fig. 6 The elements of the dictionary that we construct. Each signal is a time windowed background subtracted version of the original time history. DE: Dictionary element

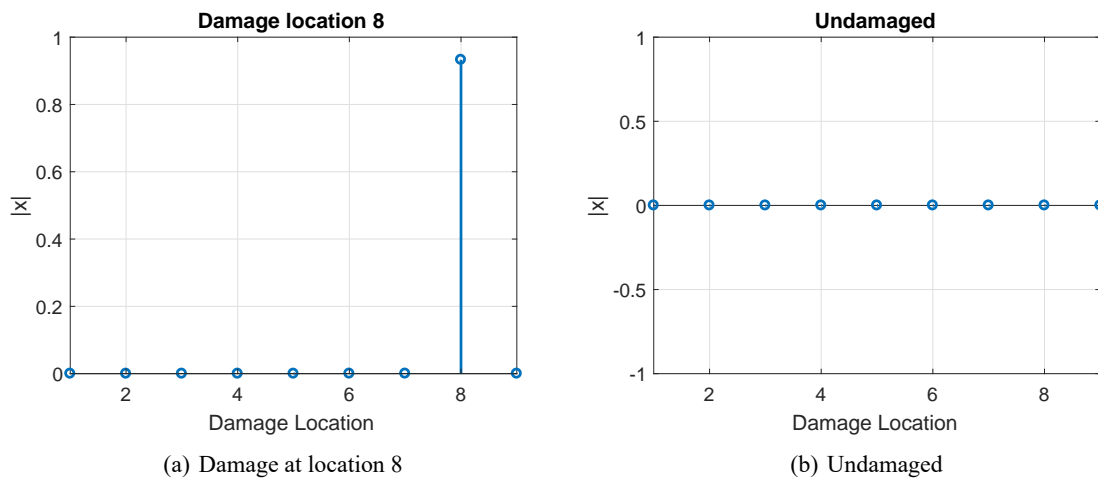


Fig. 7 Absolute values of the elements of the vector \mathbf{x} . As discussed earlier, they point to the location of the damage

4.2.2 Case 2: Test signals have multiple damages

In this case study we demonstrate the performance of the proposed algorithm when the test signals are acquired from a scenario when there are multiple damages. For this case, we assume that the effects of multiple damage may be linearly combined. This implies, if damage at locations 1 and 2 yields the background subtracted signals \mathbf{a}_1 and \mathbf{a}_2 , respectively, then the background subtracted test signal, \mathbf{y} , maybe approximated as $\mathbf{y} \approx \mathbf{a}_1 + \mathbf{a}_2$. This only holds for small damages. This assumption

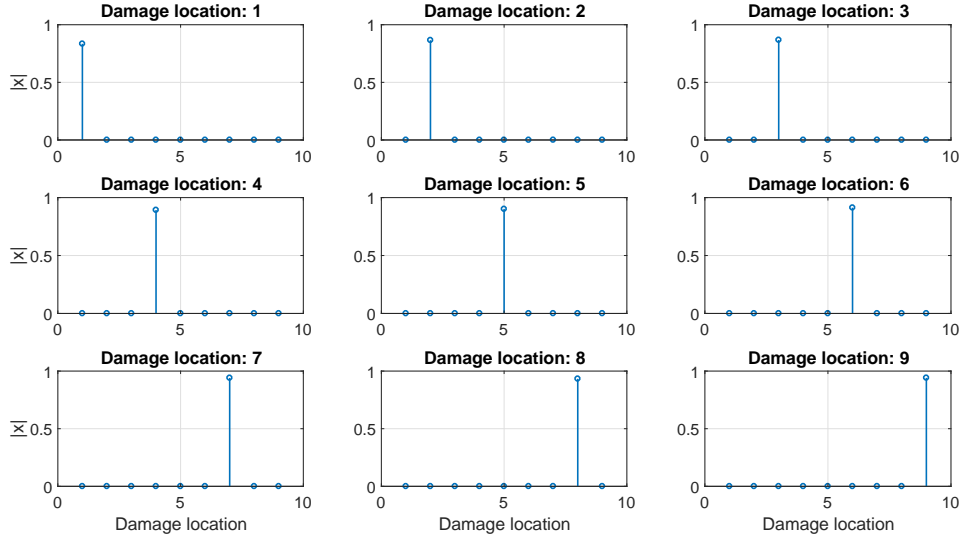


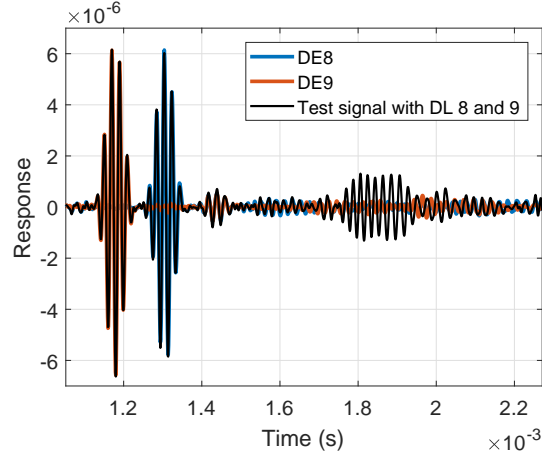
Fig. 8 The absolute value of each element of \mathbf{x} for all the 9 damage cases. Clearly, we retrieve the correct damage locations in all the cases

implies that we neglect the scattering of scattered waves from damages. For larger damage, such scattering will have significant energy. As discussed earlier, based on Fig. 5, the damage feature wave packet amplitudes are two orders of magnitude below the incident wave packet. By extrapolating this idea, we conclude that the scattering of the scattered will be at least another order of magnitude lower compared to damage feature wave packet. Typically, such low amplitudes will be shrouded by noise and hence we can neglect it.

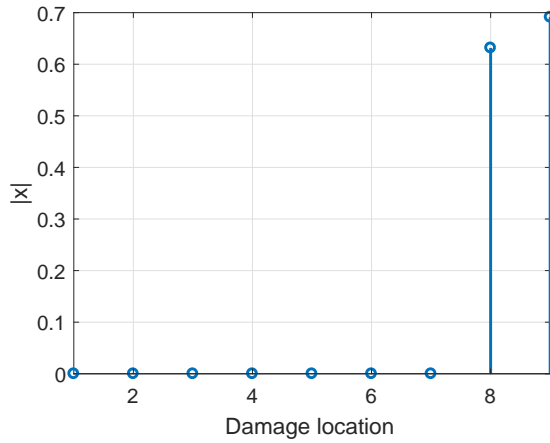
Fig. 9(a) shows a comparison of a test signal acquired from a case when the beam is damaged at locations 8 and 9 and the dictionary elements \mathbf{a}_8 and \mathbf{a}_9 . Fig. 9(b) shows the damage pointer vector, \mathbf{x} , for this case. Clearly, the assumption of linearity holds, and the proposed approach localizes damage accurately.

4.2.3 Case 3: Test signals with single damage of different extents

In this case study we demonstrate the efficacy of the proposed approach when the test signals are acquired from scenarios when the damage extent is different from the one used for dictionary construction. Fig. 11(a) compares the damage features for different damage extents at location 7 with that of the dictionary element and the undamaged signal. We observe that the wave packet has very similar characteristics with the only difference being the amplitude. Hence, we expect higher magnitudes associated with the corresponding element of the damage pointer vector, \mathbf{x} . Fig. 11(b) demonstrates this. With an increase in the damage extent the magnitude of element 7 of vector \mathbf{x} also increases. The expected magnitude of the damage pointer vector may be calibrated to damage extent for successful damage quantification.



(a)



(b)

Fig. 9 (a) A comparison of the test signal acquired from a scenario where the beam is damaged at locations 8 and 9 with the dictionary elements 8 and 9. DE: Dictionary element, DL: Damage location (b) Absolute value of the vector \mathbf{x} for the test signal shown in (a). Clearly the damage pointer vector points to locations 8 and 9

4.3 Impact of noise

In the previous subsection we demonstrate the power of harnessing the inherent sparsity of the damage detection problem. In this section, we study the impact of noise on the proposed approach, hence, showcasing the robustness. To do this, we add Gaussian white noise to the signals in the following manner

$$\tilde{\mathbf{s}} = \mathbf{s} + \sigma_{\text{noise}}\varepsilon \tag{6}$$

where $\tilde{\mathbf{s}}$ and \mathbf{s} are noisy and noise-free signals. ε is a Gaussian white noise process with each time

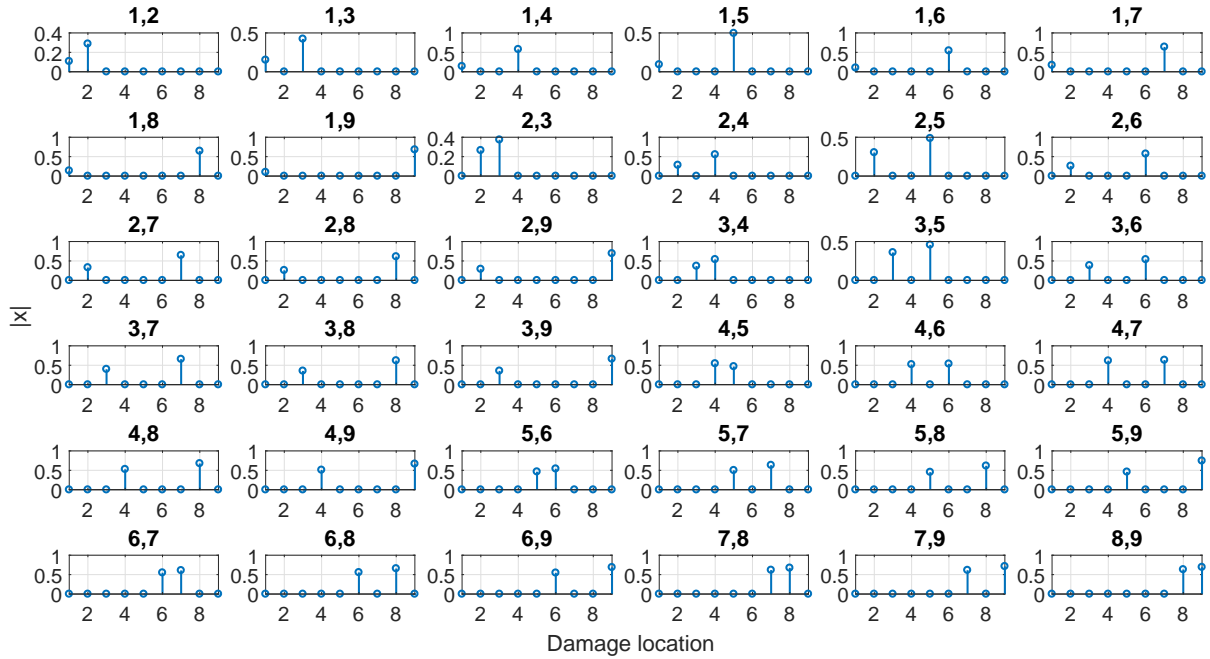


Fig. 10 The damage pointer vector elements for all possible combinations of two damages. The proposed approach accurately identifies all the multiple damages

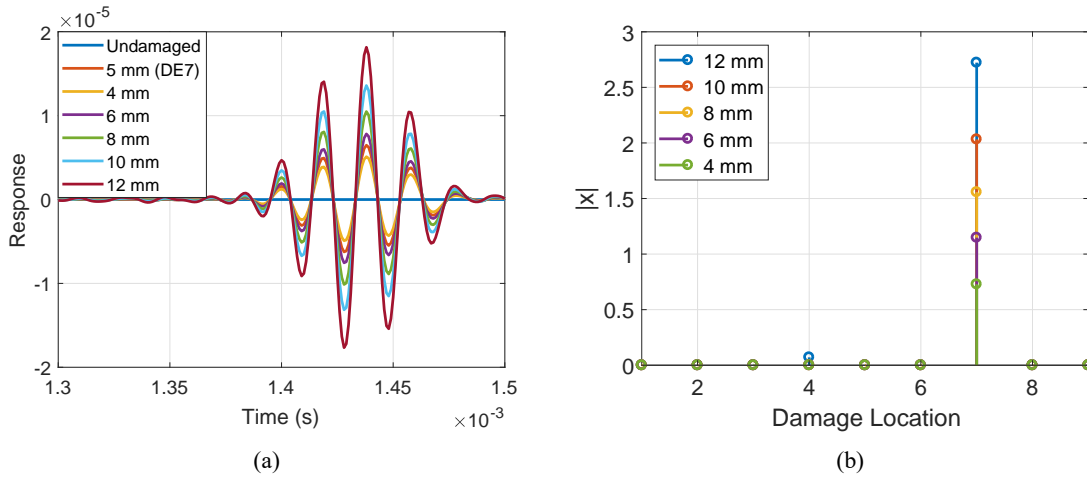


Fig. 11 (a) A comparison of the damage features produced by different intensities of damage at location 7. The crack depth captures the variation in damage intensity. The dictionary has a crack depth of 5 mm. DE7: Dictionary element 7, (b) The elements of the damage pointer vector \mathbf{x} for the signals shown in (a)

element being a Gaussian random variable with zero mean and unit variance. σ_{noise} is the intensity of noise corrupting the signal. We measure the noise intensity in terms of SNR_{dB}

$$SNR_{dB} = 20 \log_{10} \left(\frac{\mathbf{s}_{RMS}}{\varepsilon_{RMS}} \right) \tag{7}$$

where \mathbf{s}_{RMS} is the root mean square (RMS) value of the noise-free signal. ε_{RMS} is the RMS value of the added noise. For a zero mean stationary Gaussian process $\varepsilon_{RMS} = \sigma_{noise}$.

Fig. 12 shows the effect of noise on each case defined earlier. For cases 1,2 and 3 we have 9, 36 and 45 test signals respectively. For each SNR_{dB} level we solve the sparse representation problem 50 times. For each trial, we count the number of correct localizations. We define accuracy as the ratio of number of correct classifications to the total number of test signals for the case. This ensures accuracy is between 0 and 1. Taking all the 50 trials we estimate the mean and standard deviation of the accuracies. The standard deviations for case 1 is greater than that in cases 2 and 3 because of the lower number of test signals. In general, we observe very high accuracy beyond a noise level of 25 dB in all cases.

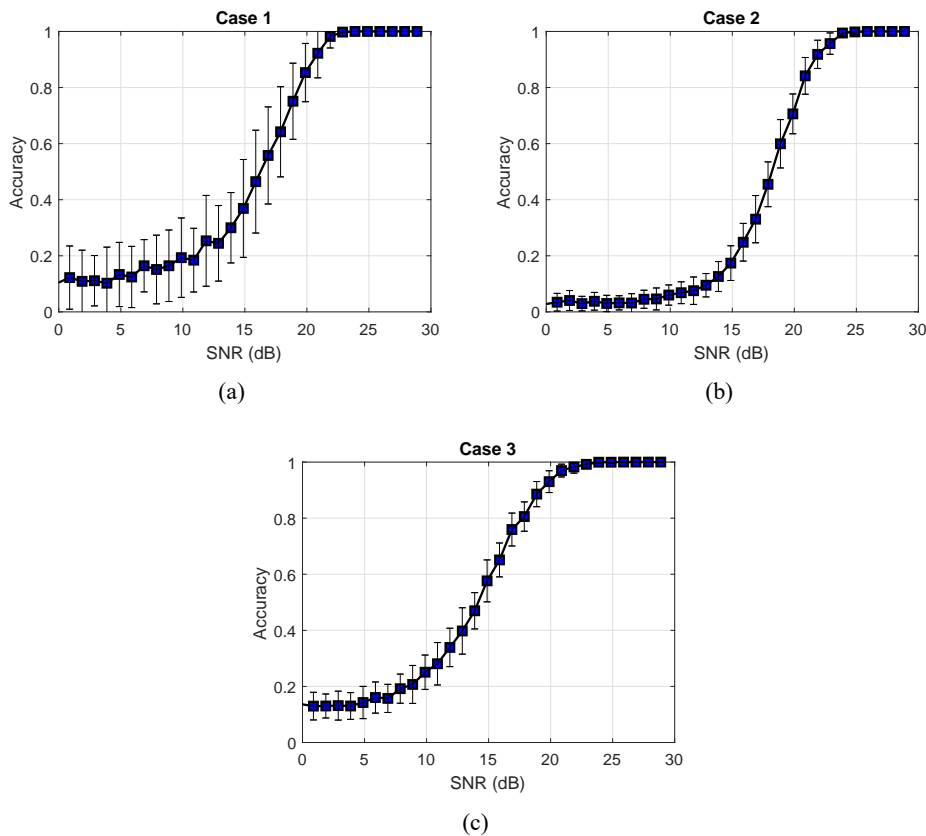


Fig. 12 Impact of noise on the performance of the proposed algorithm for (a) Case 1, (b) Case 2, (c) Case 3

5. Conclusions

In this paper we propose an approach that harnesses the inherent sparsity in the damage detection problem in beams using Lamb waves. We formulate the damage detection problem in a sparse representation framework. This involves the construction of a dictionary consisting of signals acquired from various damaged scenarios of the beam, that characterizes the damaged behavior. Subsequently, we use this dictionary for performing damage detection and localization for a signal acquired from an unknown damaged scenario, by solving a sparse regression problem. We conduct numerical simulations to demonstrate the ubiquity of the proposed framework in dealing with scenarios of multiple damage as well as various damage extents. In addition, we show that the proposed approach achieves accuracy even with noisy signals of SNR_{dB} of 25 dB.

Acknowledgments

DS and SN gratefully acknowledge the funding from Texas Instruments grant TI-168 G84040/G83198.

References

- Alleyne, D.N., Lowe, M.J.S. and Cawley, P. (1998), "The reflection of guided waves from circumferential notches in pipes", *J. Appl. Mech.*, **65**(3), 635-641.
- Baraniuk, R.G. (2007), "Compressive sensing", *IEEE Sign. Proc. Mag.*, **24**(4), 118-120, 124.
- Boller, C. (2000), "Next generation structural health monitoring and its integration into aircraft design", *J. Syst. Sci.*, **31**(11), 1333-1349.
- Candes, E. and Romberg, J. (2005), ℓ_1 *MAGIC: Recovery of Sparse Signals via Convex Programming*, Technical Report, Caltech, California, U.S.A.
- Chakraborty, A. and Gopalakrishnan, S. (2006), "A spectral finite element model for wave propagation analysis in laminated composite plate", *J. Vibr. Acoust.*, **128**(4), 477-488.
- Demma, A., Cawley, P., Lowe, M.J.S., Roosenbrand, A.G. and Pavlakovic, B. (2004), "The reflection of guided waves from notches in pipes: A guide for interpreting corrosion measurements", *NDT E Int.*, **37**(3), 167-180.
- Doyle, J.F. (1997), *Wave Propagation in Structures: Spectral Analysis Using Fast Discrete Fourier Transforms*, Springer.
- Eybpoosh, M., Berges, M. and Noh, H.Y. (2016), "Sparse representation of ultrasonic guided-waves for robust damage detection in pipelines under varying environmental and operational conditions", *Struct. Contr. Health Monitor.*, **23**(2), 369-391.
- Farrar, C.R., Doebling, S.W. and Nix, D.A. (2001), "Vibration based structural damage identification", *Philosoph. Transac. Roy. Soc. A*, **359**, 131-149.
- Farrar, C.R. and Worden, K. (2007), "An introduction to structural health monitoring", *Philosoph. Transac. Roy. Soc. A*, **365**, 303-315.
- Giurgiutiu, V. (2008), *Structural Health Monitoring: with Piezoelectric Wafer Active Sensors*, Academic Press.
- Gopalakrishnan, S., Martin, M. and Doyle, J.F. (1992), "A matrix methodology for spectral analysis of wave propagation in multiple connected Timoshenko beams", *J. Sound Vibr.*, **158**(1), 11-24.
- Gopalakrishnan, S. and Doyle, J.F. (1995), "Spectral super-elements for wave propagation in structures with local non-uniformities", *Comput. Meth. Appl. Mech. Eng.*, **121**(1-4), 77-90.
- Gopalakrishnan, S., Chakraborty, A. and Mahapatra, D.R. (2007), *Spectral Finite Element Method: Wave*

- Propagation Diagnostics and Control in Anisotropic and Inhomogenous Structures*, Academic Press.
- Gopalakrishnan, S. (2009), *Modeling Aspects in Finite Elements*, Encyclopedia of Structural Health Monitoring, John Wiley and Sons.
- Gopalakrishnan, S. and Mitra, M. (2010), *Wavelet Methods for Dynamical Problems: With Applications to Metallic, Composite and Nano-Composite Structures*, CRC Press.
- Graff, K.F. (1991), *Wave Motion in Elastic Solids*, Dover Publications.
- Hastie, T., Tibshirani, R. and Friedman, J. (2009), *The Elements of Statistical Learning: Data Mining, Inference and Prediction*, Springer.
- Hernandez, E.M. (2014), "Identification of isolated structural damage from incomplete spectrum information using ℓ_1 -norm minimization", *Mech. Syst. Sign. Proc.*, **46**, 59-69.
- Hu, N., H Fukunaga, H., Kameyama, M., Mahapatra, D.R. and Gopalakrishnan, S. (2007), "Analysis of wave propagation in beams with transverse and lateral cracks using a weakly formulated spectral method", *ASME J. Appl. Mech.*, **74**(1), 119-127.
- Igawa, H., Komatsu, K., Yamaguchi, I. and Kasai, T. (2004), "Wave propagation analysis of frame structures using the spectral element method", *J. Sound Vibr.*, **277**, 1071-1081.
- Kandel, B.M., Wolk, D.A., Gee, J.C. and Avants, B. (2013), *textitPredicting Cognitive Data from Medical Images Using Sparse Linear Regression*, Lecture Notes in Computer Science, Springer, Berlin, Heidelberg, Germany, **7197**.
- Kim, S.J., Koh, K., Lustig, M., Boyd, S. and Gorinevsky, D. (2007), "A method for large-scale ℓ_1 -regularized least squares", *IEEE J. Select. Top. Sign. Proc.*, **1**(4), 606-617.
- Kumar, D.S., Chakraborty, A. and Gopalakrishnan, S. (2004), "A spectral finite element for wave propagation and structural diagnostic analysis of composite beam with transverse crack", *Fin. Elem. Analy. Des.*, **40**(13-14), 1729-1751.
- Levine, R.M. and Michaels, J.E. (2013), "Model-based imaging of damage with Lamb waves via sparse reconstruction", *J. Acoust. Soc. Am.*, **133**(3), 1525-1534.
- Liu, Z. and Kleiner, Y. (2012), "State-of-the-Art Review of Technologies for Pipe Structural Health Monitoring", *IEEE Sens. J.*, **12**(6), 1987-1992.
- Liu, C., Harley, J.B., Berges, M., Greve, D.W. and Oppenheim, I.J. (2015), "Robust ultrasonic damage detection under complex environmental conditions using singular value decomposition", *Ultrason.*, **58**, 75-86.
- Lowe, M.J.S., Alleyne, D.N. and Cawley, P. (1998), "Defect detection in pipes using guided waves", *Ultrason.*, **36**(1-5), 147-154.
- Lu, Y., Ye, L., Su, Z., Zhou, L. and Cheng, L. (2007), "Artificial neural network (ANN)-based crack identification in aluminum plates with lamb wave signals", *J. Intell. Mater. Syst. Struct.*, **20**, 39-49.
- Lu, Y. and Michaels, J.E. (2008), "Numerical implementation of matching pursuit for the analysis of complex ultrasonic signals", *IEEE Trans. Ultrason. Ferroelectr. Freq. Contr.*, **55**(1), 173-182.
- Murthy, M.V.V.S., Gopalakrishnan, S. and Nair, P.S. (2011), "Signal wrap-around free spectral element formulation for multiply connected finite 1-D waveguides", *J. Aerosp. Sci. Technol.*, **63**(1), 72-88.
- Na, W.B. and Kundu, T. (2002), "Underwater pipeline inspection using guided waves", *Trans. ASME*, **124**, 196-200.
- Nagarajaiah, S. and Yang, Y. (2017), "Modeling and harnessing sparse and low-rank data structure: A new paradigm for structural dynamics, identification, damage detection, and health monitoring", *Struct. Contr. Health Monitor.*, **24**(1), e1851.
- Ostachowicz, W., Kudela, P., Krawczuk, M. and Zak, A. (2012), *Guided Waves in Structures for SHM: The Time-Domain Spectral Element Method*, Dover Publications.

- Ou, J. and Li, H. (2010), "Structural health monitoring in mainland China: Review and future trends", *Struct. Health Monitor.*, **9**(3), 219-241.
- Packo, P., Bielak, T., Spencer, A.B., Staszewski, W.J., Uhl, T. and Worden, K. (2012), "Lamb wave propagation modelling and simulation using parallel processing architecture and graphical cards", *Smart Mater. Struct.*, **21**, 13.
- Park, M.H., Kim, I.S. and Yoon, Y.K. (1996), "Ultrasonic inspection of long steel pipes using lamb waves", *NDT E Int.*, **29**(1), 13-20.
- Patera, A.T. (1984), "A spectral element method for fluid dynamics: Laminar flow in a channel expansion", *J. Comput. Phys.*, **54**, 468-488.
- Raghavan, A. and Cesnik, C.E.S (2007), "Review of guided-wave structural health monitoring", *Shock Vibr. Dig.*, **39**(2), 91-114.
- Rose, J.L. (1999), *Ultrasonic Waves in Solid Media*, Cambridge University Press.
- Rose, J.L. (2004), "Ultrasonic Guided Waves in Structural Health Monitoring", *Key Eng. Mater.*, **270-273**, 14-21.
- Rytter, A. (1993), "Vibration based inspection of civil engineering structures", Ph.D. Dissertation, Aalborg University, Denmark.
- Tibaduiza, D.A., Torres-Arredondo, M.A., MUjica, L.E., Rodellar, J. and Fritzen, C.P. (2013), "A study of two unsupervised data driven statistical methodologies for detecting and classifying damages in structural health monitoring", *Mech. Syst. Sign. Proc.*, **41**(1-2), 467-484.
- Tibshirani, R. (1996), "Regression shrinkage and selection via the LASSO", *J. Roy. Stat. Soc. B*, **58**(1), 267-288.
- Tse, P.W. and Wang, X. (2013), "Characterization of pipeline defect in guided-waves based inspection through matching pursuit with the optimized dictionary", *NDT E Int.*, **54**, 177-182.
- Worden, K. and Manson, G. (2007), "The application of machine learning to structural health monitoring", *Philosoph. Trans. Roy. Soc. A*, **365**, 515-537.
- Yang, Y. and Nagarajaiah, S. (2013), "Output-only modal identification with limited sensors using sparse component analysis", *J. Sound Vibr.*, **332**(19), 4741-4765.
- Yang, A., Ganesh, A., Zhou, Z., Sastry, S. and Ma, Y. (2010), textitFast ℓ_1 minimization algorithms and an application in robust face recognition: a review, Technical Report, UC Berkeley, California, U.S.A.
- Yang, Y. and Nagarajaiah, S. (2014), "Structural damage identification via a combination of blind feature extraction and sparse representation classification", *Mech. Syst. Sign. Proc.*, **45**(1), 1-23.
- Yang, Y. and Nagarajaiah, S. (2014), "Blind identification of damage in time-varying systems using independent component analysis with wavelet transform", *Mech. Syst. Sign. Proc.*, **47**(1-2), 3-20.
- Ying, Y., Garrett Jr, J.H., Harley, J., Oppenheim, I.J., Shi, J. and Soibelman, L. (2013), "Damage detection in pipes under changing environmental conditions using embedded piezoelectric transducers and pattern recognition techniques", *J. Pipeline Syst. Eng. Prac.*, **4**(1), 17-23.
- Ying, Y., Garrett Jr, J.H., Oppenheim, I.J., Soibelman, L., Harley, J., Shi, J. and Jin, Y. (2013), "Toward data-driven structural health monitoring: Application of machine learning and signal processing to damage detection", *J. Comput. Civil Eng.*, **27**(6), 667-680.
- Yu, L., Giurgiutiu, V., Wang, J. and Shin, Y.J. (2011), "Corrosion detection with piezoelectric wafer active sensors using pitch-catch waves and cross-time-frequency analysis", *Struct. Health Monitor.*, **11**(1), 83-93.